AIAA SciTech Forum
23-27 January 2023, National Harbor, MD & Online
AIAA SCITECH 2023 Forum

10.2514/6.2023-1489

Frictional Ignition of Metals in High Pressure Oxygen: A Critical Reassessment of NASA Test Data

Andres Garcia Jimenez* and Zachary Cordero ‡
Massachusetts Institute of Technology, Cambridge, MA, 02139

In this paper we develop a material index for selecting alloys resistant to frictional ignition in high pressure oxygen environments. A previous ignition-resistance metric proposed by NASA WSTF varies strongly and unpredictably with test conditions, thus limiting its usefulness. The material index developed here incorporates key material properties that strongly influence ignition behaviors, including friction coefficient, ignition temperature, and thermal effusivity. Finite element simulations were used to compute ignition temperatures for 15 alloys based on published frictional ignition data from NASA White Sands Testing Facility (WSTF). These values were used with the material index to construct property diagrams for ranking the materials based on their intrinsic frictional ignition resistance. The results demonstrate that nickel-based superalloys with low iron content are less likely to ignite under frictional heating than ferrous alloys and nickel-based superalloys with high content iron. The material index is then used to predict material performance outside of the test conditions, highlighting the effect of ambient temperature on nominal ignition resistance. We conclude by developing an empirical relation between ignition temperature and enthalpy of oxidation which can guide design of new ignition-resistant alloys.

I. Nomenclature

α	=	heat partition coefficient
μ	=	friction coefficient
ω	=	radial speed, rad/s
ρC_p	=	heat capacity, J/m^{3}K
κ	=	thermal conductivity, W/mK
e	=	surface emissivity
ΔH_{ox}	=	enthalpy of oxidation, kJ/mol
MI	=	material index
P	=	contact pressure, MPa
q	=	heat flux, W/m^2
r	=	radius, m
T	=	temperature, K
t	=	time, s
v	=	sliding speed, m/s

II. Introduction

The oxidizer-rich staged combustion (ORSC) and full-flow staged combustion (FFSC) rocket engines currently being developed by SpaceX, Blue Origin, and other US contractors offer dramatic improvements in fuel efficiency and thrust over the conventional gas generator engine cycle [1]. These power cycles both use oxidizer-rich turbopumps powered by an oxidizer-rich stream of combustion gases which burns with the remaining fuel in the main combustion chamber. ORSC and FFSC engines use propellant efficiently without sacrificing thrust because of their high chamber pressures and because all the propellant is

*Graduate Student, Department of Aeronautics and Astronautics, 77 Massachusetts Avenue, Cambridge, MA 02139, AIAA Student Member
‡Boeing Assistant Professor, Department of Aeronautics and Astronautics, 77 Massachusetts Avenue, Cambridge, MA 02139, AIAA Member

exhausted through the nozzle [1-3]. However, the increased pressure and additional turbomachinery requirements introduce new challenges, such as an increased risk of metal ignition and burning [4-6]. Frictional heating due to rubbing of rotating components (e.g., between turbine blades and the blade track) is one of the ignition mechanisms of greatest concern and is believed to have caused two recent launch failures, Sea Launch's NSS-8 and Orbital's Orb-3. Frictional ignition was studied experimentally in the 1980's and 1990's by NASA White Sands Testing Facility (WSTF) using a specialized frictional ignition rig [7]. A key outcome of this work was a quantitative ranking of ignition resistance based on the product of sliding speed v and contact pressure P at ignition [8]. While a material with a higher Pv product will take longer to ignite, it is a grouping of test parameters, not intrinsic material properties. Hence, the Pv product can vary strongly with test conditions (e.g., O_2 partial pressure, ambient temperature), limiting its utility when selecting materials for operating conditions outside those tested [8]. A more general approach for assessing the relative frictional ignition resistance of different materials is with a material index [9], a grouping of material properties whose extremal value maximizes performance, which, in this case, is ignition resistance. In this paper we discuss the limitations of the Pv product, quantitatively reassess the published NASA WSTF frictional ignition experiments, and finally use our findings to develop a material index for high pressure oxygen environments.

III. Review of NASA WSTF frictional ignition results

The NASA WSTF frictional ignition tests were carried out using a specialized rub rig depicted in **Figure 1**. Details of the apparatus, test conditions, and specimen geometries are given in [7]. During testing, two tubular specimens were rubbed against each other in a static high-pressure O_2 environment. The stator was fixed to the wall of the pressure vessel; the rotor was attached to the shaft assembly. The shaft speed was 17000 rpm, corresponding to a linear sliding speed of 22 m/s, and the contact force was ramped at a fixed rate of 31 N/s. These conditions were used to assess the frictional ignition behaviors of the alloys listed in **Table 1** [8].

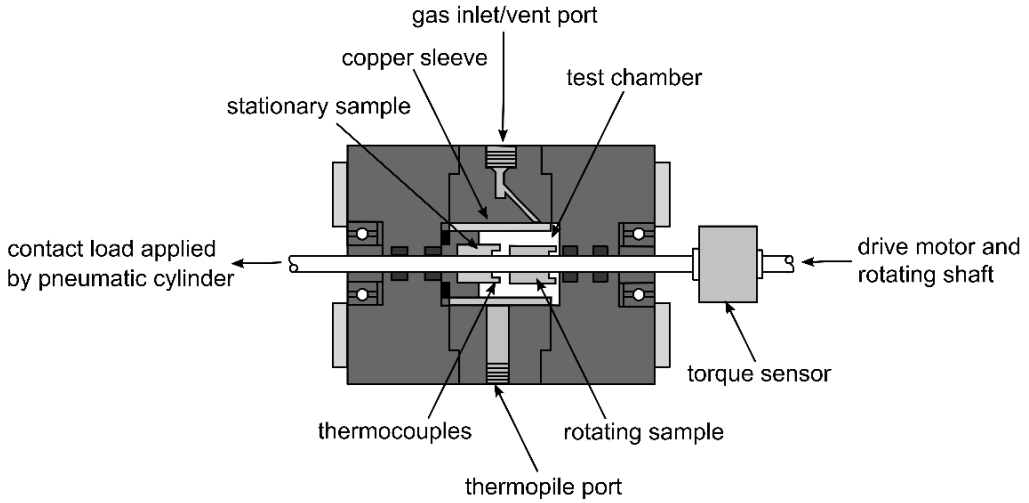

Figure 1: WSTF frictional ignition testing rig set-up. Adapted from [7].

Table 1: Alloys tested in WSTF frictional ignition test campaign.

Alloy	Weight Percent												
	Ni	Fe	Cr	Cu	Al	Mo	Mn	W	Co	Nb	Ta	Ti	Other
Ni 200	99	0.3		0.3									
Haynes 214	77	3	16		4								0.2 Y

Alloy	Weight Percent												
	Ni	Fe	Cr	Cu	Al	Mo	Mn	W	Co	Nb	Ta	Ti	Other
IN 600	76	9	15	0.1									
IN MA6000	69		15		5	3		4			2	2	1.1 Y_2O_3
MK500	63	2		30	3		2					0.5	
Waspaloy	58		21		1	4			16			2	
Haynes 230	55	3	22		0.2	2	0.2	14	3				
IN 718	53	19	19		0.4	3				5		0.9	
Hastelloy X	48	19	22			9		0.6	1				
IN 706	42	36	16	0.3	0.4		0.4		3			2	
Incoloy 903	38	42			0.9				15	1		3	
Incoloy 909	38	42							13	5		2	
SS 304	9	72	19										
IN MA956		74	20					5				0.5	
SS 440C		82	17										1 C

The friction coefficient μ was measured over the course of each frictional ignition experiment [8]. For all materials tested, the friction coefficient decreased rapidly during the first few seconds of the test then plateaued towards a steady-state value [7,10,11]. Stoltzfus et al. attributed the decrease in friction coefficient to the growth of a lubricating oxide at the rubbing interface [7,12]. The steady-state friction coefficient and ignition time of each alloy are summarized in **Table 2**.

Table 2: Steady-state friction coefficient μ, ignition time, and Pv product of alloys tested in [8].

Alloy	Friction Coefficient, μ	Ignition Time, t_{ign} (s)	Average Pv Product ($W/m^2 \times 10^{-8}$)
Ni 200	0.072	88	3.05
Haynes 214	0.046	88	3.05
IN 600	0.038	72	2.50
IN MA6000	0.028	66	2.28
MK500	0.042	59	2.03
Waspaloy	0.035	45	1.55
Haynes 230	0.12	43	1.50
IN 718	0.038	38	1.30
Hastelloy X	0.092	35	1.20
IN 706	0.077	32	1.12
Incoloy 903	0.018	31	1.07
Incoloy 909	0.10	30	1.04
SS 304	0.034	29	1.0
IN MA956	0.065	20	0.68
SS 440C	0.25	18	0.62

Stoltzfus et al. ranked the frictional ignition resistance of different materials based on the product of sliding speed v and contact pressure P at ignition [7,8]. Their reasoning was that Pv is directly proportional to the frictional heat flux (q) through the friction coefficient,

$$q = \mu P v. \tag{1}$$

Thus, higher Pv values mean a higher interfacial heat flux is required to drive ignition [7,8,12]. **Table 2** shows the alloys ranked according to their Pv values.

A major limitation of using Pv to rank frictional ignition resistance is that it varies strongly with test conditions. For instance, Stoltzfus et al. observed that the Pv values for a given material have a complicated non-monotonic dependence on oxygen pressure, first decreasing then increasing with increasing oxygen pressure [8]. Thus, the ranking given in **Table 2** is likely only valid for a specific set of test conditions; changing parameters such as the oxygen pressure, ambient temperature, sliding speed, loading rate, etc. might cause the ranking to change in unpredictable ways.

IV. Material index for frictional ignition resistance

An alternative approach to material selection is to develop a material index that reflects intrinsic resistance to frictional ignition. This approach is advantageous in that material indices are not limited to a specific set of test conditions. Test data can be used to determine a material index for ignition resistance under one set of conditions, which is then easily generalized to other conditions without further experiments. To develop a material index for frictional ignition resistance, we first recognize that our objective is always to maximize the ignition time, t_{ign}, regardless of the sliding conditions. Approximating the frictional ignition specimen as a 1D semi-infinite body with a constant heat flux boundary condition q, the time to a reach a given increment in interfacial temperature ΔT is

$$t = \left(\frac{1}{q}(\Delta T)\sqrt{\rho C_p \kappa}\right)^2, \tag{2}$$

where $\sqrt{\rho C_p \kappa}$ is the thermal effusivity. The frictional heat flux q is given by

$$q = \alpha \mu P v, \tag{3}$$

where α is the heat partition coefficient. Assuming the specimen has an initial uniform temperature T_0 and a material-specific ignition temperature T_{ign}, the temperature increment at ignition is

$$\Delta T = (T_{ign} - T_0). \tag{4}$$

Combining **Equations 2-4** gives the objective function

$$t_{ign} = \left(\frac{1}{\alpha P v}\right)^2 \left[\frac{(T_{ign} - T_0)\sqrt{\rho C_p \kappa}}{\mu}\right]^2. \tag{5}$$

Inspection of **Equation 5** shows that we can maximize t_{ign} by maximizing the material index

$$MI = \left[\frac{1}{\mu}(T_{ign} - T_0)\sqrt{\rho C_p \kappa}\right]^2. \tag{6}$$

Accordingly, in selecting ignition-resistant materials, we seek materials with a high ignition temperature, high thermal effusivity, and low friction coefficient. Note that here we assume T_{ign} and μ are independent of test conditions. In reality, the friction coefficient can depend on sliding speed, contact pressure, and the specific rotor/stator pair in case of dissimilar material combinations [7,8,12]. However, such effects are expected to be minor under the ranges of oxygen pressures and sliding speeds relevant to oxygen-rich turbomachinery.

V. Calculations of frictional ignition temperature

Using this material index, we rank the frictional ignition resistance of the alloys summarized in **Table 1**. The friction coefficient and thermal effusivity of these different materials are available in the open literature. To determine the ignition temperature, we used finite element analysis to compute the

temperature field within the test specimens during the WSTF frictional ignition experiments. These simulations were carried out using the COMSOL Multiphysics software [13]. **Figure 2** depicts the simulation domain, which was bounded by the inner wall of the pressure vessel and included the stator, specimen insulator (M400), and specimen mount (MK500). The latter two elements were included because heat diffused into the specimen mount during experiments on ignition-resistant alloys. Fully 3D finite element simulations were used because of the asymmetry of the mount. The domain surrounding the specimen was modeled as gaseous O_2, using published thermal properties at a pressure of 6.8 MPa [14]. The temperature profile was computed by solving the heat equation, considering heat conduction in the solids and gaseous O_2 and accounting for radiative heat transfer between the solid surfaces and temperature-dependent material properties. There was no interfacial thermal resistance at the gas/solid interface. The room-temperature material properties which included the density ρ, thermal conductivity κ, specific heat capacity C_p, and emissivity e, are summarized in **Table 3**.

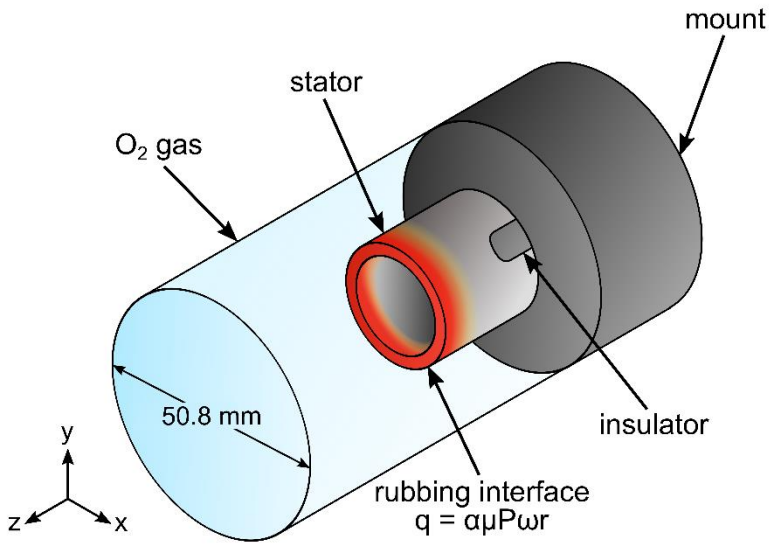

Figure 2: Model setup of frictional heating in COMSOL Multiphysics.

Table 3: Material properties at room temperature of the different materials used in the FEM model.

Alloy	ρ (kg/m^3)	κ (W/(m·K))	C_p (J/(kg·K))	e
Ni 200	8890	71.0	458	0.5
Haynes 214	8050	12.0	452	0.6
IN 600	8470	12.5	444	0.6
IN MA6000	8110	10.8	394	0.5
MK500	8160	11.0	520	0.5
Waspaloy	8440	17.5	419	0.4
Haynes 230	8970	8.9	397	0.5
IN 718	8190	11.4	435	0.3
Hastelloy X	8220	9.2	487	0.5
IN 706	8050	12.5	444	0.5
Incoloy 903	8250	16.9	442	0.5
Incoloy 909	8190	14.8	427	0.5
SS 304	8000	16.2	500	0.5

Alloy	ρ (kg/m^3)	κ (W/(m·K))	C_p (J/(kg·K))	e
IN MA956	7250	10.9	469	0.5
SS 440C	7800	10.2	460	0.5

The entire domain was assigned an initial temperature of 298 K. Frictional heating was modeled as a heat flux boundary condition at the rubbing interface:

$$q = \alpha \mu P \omega r, \tag{7}$$

where ω is angular speed (1780 rad/s), r is radial distance, P is contact pressure, and α is the heat partition coefficient, corresponding to the fraction of frictional heat diffusing into the stator. Here we assume α = 1/2, meaning the frictional heat partitions evenly between the rotor and stator. The model did not consider enthalpy of oxidation because its effect is minor prior to ignition. The sides of the simulation domain were assigned fixed temperature boundary conditions (T = 298 K).

The predicted interfacial temperature for MK500 is plotted as a function of time in **Figure 3**. The interfacial temperature increases monotonically to the ignition temperature of 1420 K. This ignition temperature is consistent with a previous 1D finite element model of frictional ignition of MK500 which did not consider radiative heat losses or temperature-dependent material properties [15]. The form of the MK500 interfacial temperature v. time curve is similar to those of the other materials analyzed here.

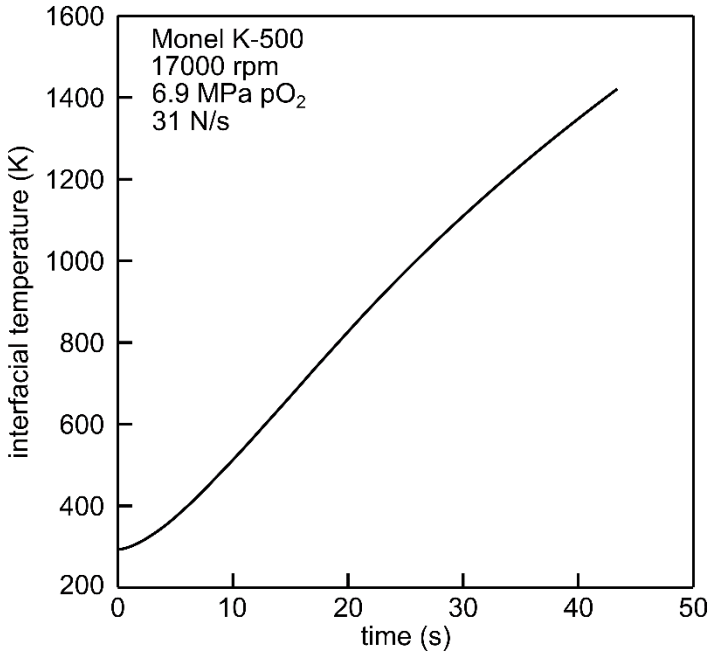

Figure 3: Interfacial temperature of Monel K-500 during frictional ignition testing.

Figure 4 summarizes the ignition temperature data for all materials tested in the original WSTF frictional ignition campaign [8]. Nickel-based superalloys with low-iron content (e.g., Haynes 214, IN600, MA6000, etc.) tend to ignite at later times and at higher interfacial temperatures. The cupronickel alloy MK500 exhibits only moderate frictional ignition resistance despite its low flammability as assessed through promoted combustion testing [8,16]. The alloys that ignite most readily are those that contain higher Fe concentrations (e.g., IN718, IN706, etc.). Nickel-based alloys with high Fe content ignite at very early times (18 – 35 s) and at low temperatures (500 – 1000 K). Ferrous alloys (e.g., stainless steels) are the least ignition resistant, igniting in as little as 20s, consistent with their high flammability in promoted combustion testing [17,18].

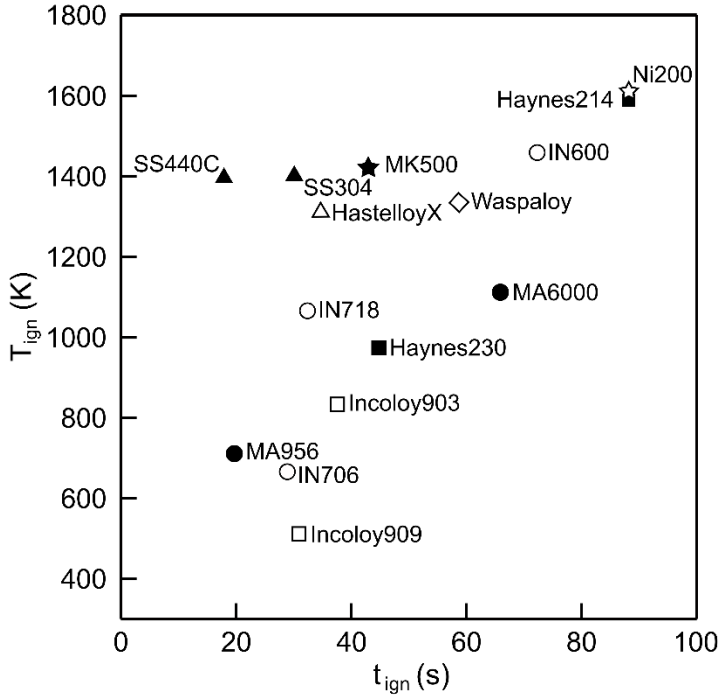

Figure 4: Ignition temperature v. ignition time for all materials tested.

VI. Trends in frictional ignition resistance

Figure 5a is a property diagram for frictional ignition resistance with T_0 = 298 K. Visualizing the data in this way makes it easier to compare the ignition resistance of different materials. Specifically, the dashed lines indicate material index iso-contours; materials that lie along the same iso-contour will ignite at the same time. Ignition-resistance increases moving towards the bottom-right corner of this property diagram. Note that the locations of the individual materials depend strongly on ambient temperature. For example, **Figure 5b** is a property diagram for T_0 = 500 K. Compared to **Figure 5a**, the individual datapoints have shifted leftwards. The shift is greater for materials with lower ignition temperatures, highlighting their sensitivity to slight increases in initial temperature. This effect is most obvious when comparing SS304 and Incoloy 909 – these materials have a similar material index at T_0 = 298 K but Incoloy 909 is clearly much more susceptible to frictional ignition when T_0 increases by just 200 K. Quantitatively assessing the effect of ambient temperature on ignition-resistance is impossible with the Pv product but is straightforward with the present material index.

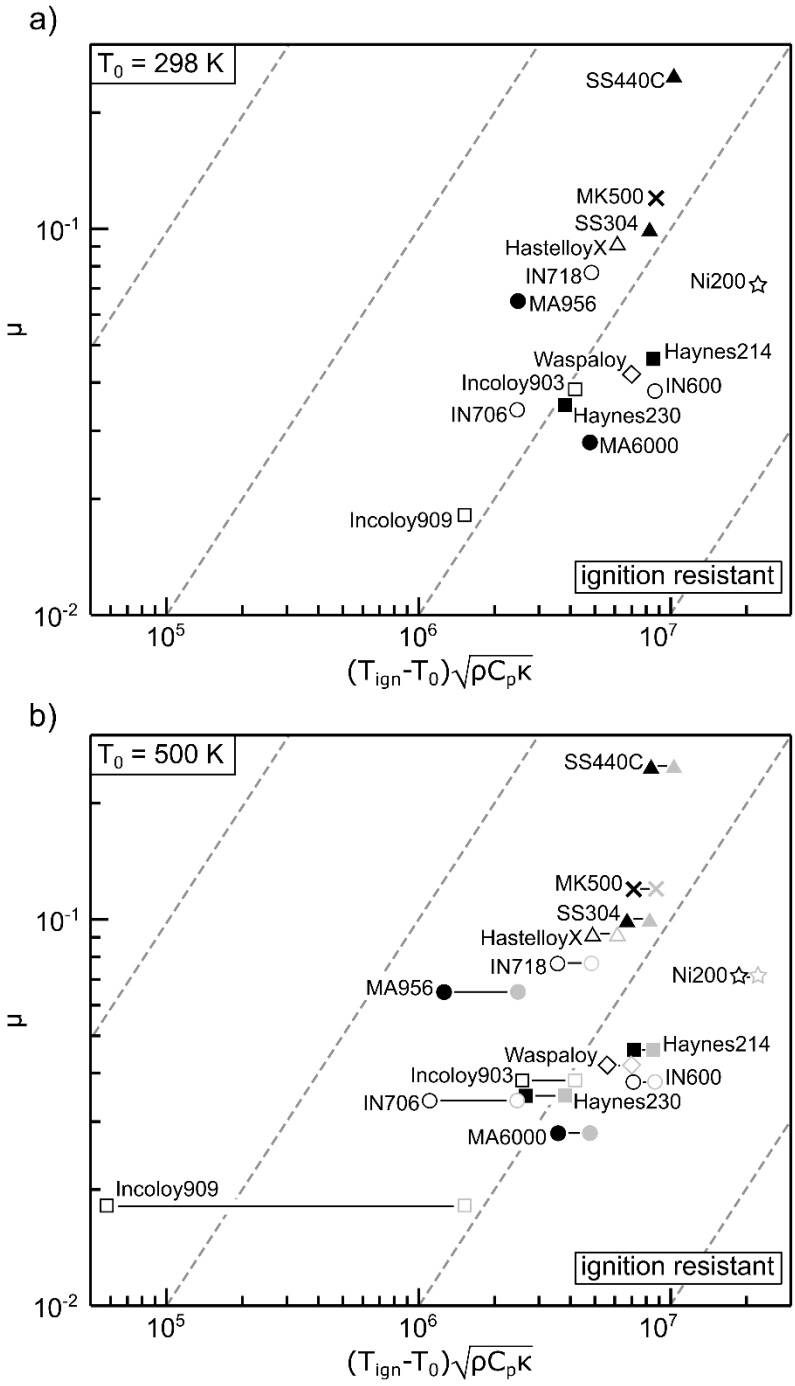

Figure 5: Frictional ignition property diagrams with (a) T_0 = 298 K and (b) T_0 = 500 K. In (b), datapoints in grey correspond to values with T_0 = 298 K.

Figure 6 compares the Pv and material index values of each alloy. There is a positive correlation between the two parameters – materials with a high Pv value also tend to have a high material index. However, there are important differences. Namely materials with similar Pv values can have noticeably different material indices (Haynes 214 v. Ni200) and vice versa (Incoloy 903 v. Haynes 230).

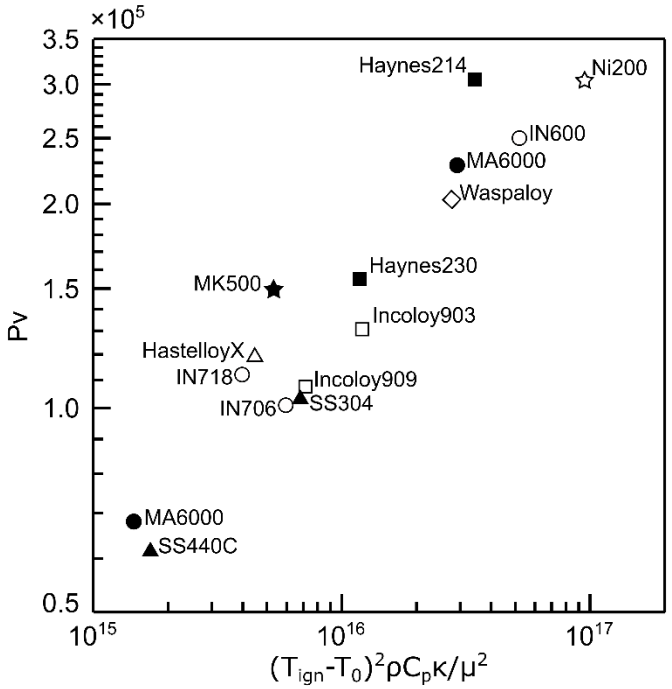

Figure 6: Comparison of frictional ignition resistance ranking obtained from the Pv product and material index.

Flammability of metals is commonly measured using promoted combustion experiments and quantified in two ways: O_2 pressure threshold (maximum O_2 pressure under which a material does not sustain combustion) and burn rate, which are crucial guidelines when considering the selection and design of materials for high pressure oxygen applications [8,19-21]. However, flammability of metals should not be the only consideration. For instance, Ni200, Haynes 214, and MK500 have O_2 pressure thresholds greater than 69 MPa [8,20], but ignite under frictional ignition under pressures below 6.9 MPa [7,8,10]. Further, when comparing ignition resistance from our material index with the burn rate at the same pO_2 of 6.9 MPa as shown in **Figure 7**, we generally observe that flammable materials ignite readily with some important exceptions. For example, under the same O_2 pressure, we observe that MK500 has a moderate ignition resistance and does not burn in promoted combustion experiments while IN600 has a high ignition resistance and burns. Consequently, ignition resistance should be carefully considered in the design and selection of materials for high O_2 pressure applications and the quantification of ignition resistance with our material index can aid in the selection of materials for these environments.

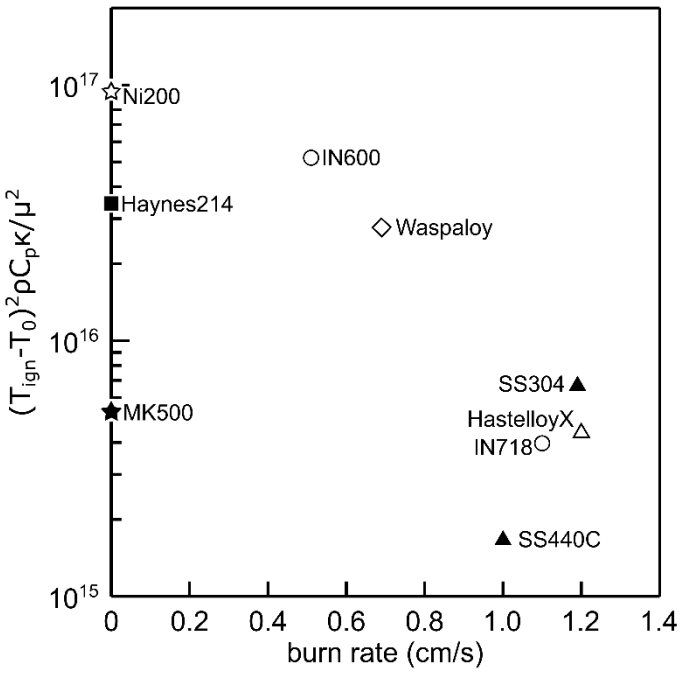

Figure 7: Material index for frictional ignition resistance of select materials v. burn rate obtained from promoted combustion experiments at pO_2 = 6.9 MPa [8,19-21].

Another consideration in the design of materials is the enthalpy of oxidation. Models of thermal ignition show that ignition temperature corresponds to the point in which the overall rate of heat loss is less than the heat generated during oxidation, which is proportional to the enthalpy of oxidation and oxidation rate [22,23]. This indicates that alloys with higher enthalpies of oxidation and faster oxidation rates will tend to have lower ignition temperatures. We observe this trend by plotting the frictional ignition temperature v. the enthalpy of oxidation of each of the alloys as shown in **Figure 8**. The enthalpies of oxidation were calculated using the FactSage free energy minimization software (with FTOxid, FactPS, and FSstel databases) [24]. Alloys (MK500, Ni200, and others) with high ignition temperatures in the range of 1400 – 1600 K have low enthalpies of oxidation (200 – 250 kJ/mol) while alloys such as MA956 and IN706 have ignition temperatures below 750 K and high enthalpies of oxidation (350 – 450 kJ/mol). Based on this trend, we developed an empirical relationship given by

$$T_{ign} = -2.97 \left[\frac{\text{mol·K}}{\text{kJ}}\right] |\Delta H_{ox}| + 2120 \text{ [K]}, \quad (8)$$

to estimate the ignition temperature based on the enthalpy of oxidation. This empirical relationship only provides an approximate value of the ignition temperature, but can guide the design of new alloys considering that lower enthalpies of oxidation result in higher ignition temperatures, favoring higher ignition resistance.

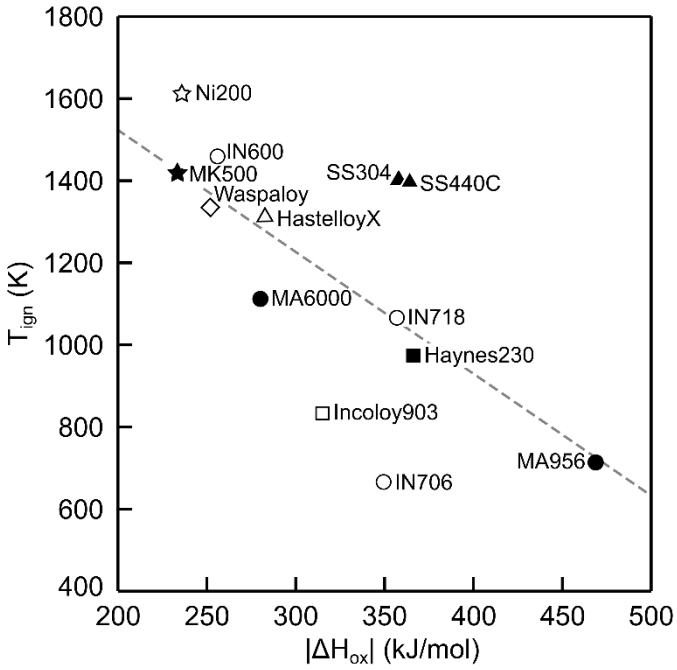

Figure 8: Ignition temperature v. enthalpy of oxidation at T_0 = 300 K with best fit overlaid.

VII. Conclusions

The NASA metric for assessing frictional ignition resistance is limited to a specific set of test conditions. By contrast, the material index developed here is a grouping of material properties – ignition temperature, friction coefficient, thermal effusivity – that can be used to assess ignition resistance under essentially any conditions. Materials with the same material index will ignite at the same time under a given set of sliding conditions, and the ignition time scales linearly with the material index. The material index shows that ignition resistant alloys have a low friction coefficient, high ignition temperature, and high thermal effusivity. Finite element simulations of the NASA WSTF frictional ignition were used to compute the ignition temperatures of 15 alloys. These results were integrated with the material index to reveal the following key trends:

- Nickel-based superalloys with low iron content are more ignition resistant and ignite at higher temperatures than ferrous and nickel-based superalloys with high content iron.
- Alloys that are less flammable tend to be more ignition-resistant; however, there are some important exceptions. For example, MK500 and Haynes 214 will ignite under high speed sliding but do not burn in promoted combustion tests.
- Materials with low ignition temperatures are more sensitive to changes in initial temperature condition.
- Ignition temperature decreases with increasing enthalpy of oxidation, in line with classical ignition theory. An empirical correlation between enthalpy of oxidation and ignition temperature was developed to guide design of new ignition resistant materials.

References

[1] Peery, S. D., and Parsley, R. C., "Merits of full flow vs. conventional staged combustion cycles for reusable launch vehicle propulsion," AIP Conference Proceedings, 1996.

[2] Davis, J., "Advantages of a full-flow staged combustion cycle engine system," 33rd Joint Propulsion Conference and Exhibit, 1997.
[3] Katorgin, B., Chvanov, V., Chelkis, F., Lozino-Lozinskaya, I., and Tanner, L., "Oxidizer-rich staged combustion rocket engines use and development in Russia," Space Programs and Technologies Conference, 1995.
[4] Clark, A. F., and Hust, J. G., "A review of the compatibility of structural materials with oxygen," AIAA Journal, Vol. 12, 1974, pp. 441–454.
[5] Stoltzfus, J. M., "Test methods for determining the suitability of metal alloys for use in oxygen enriched environments," NASA 2nd National Technology Transfer Conference and Exposition, Vol. 1, 1991, pp. 183-192.
[6] Jacinto, M., "The need for oxygen compatible materials," 35th Joint Propulsion Conference and Exhibit, 1999.
[7] Benz, F. J., and Stoltzfus, J. M., "Ignition of Metals and Alloys in Gaseous Oxygen by Frictional Heating," Flammability and Sensitivity of Materials in Oxygen-Enriched Atmospheres, Vol. 2, 1986, pp. 16-37.
[8] Stoltzfus, J. M., Benz, F. J., and Homa, J., "The Pv Product Required for the Frictional Ignition of Alloys," Flammability and Sensitivity of Materials in Oxyqen-Enriched Atmospheres, Vol. 4, 1989.
[9] Ashby, M. F., *Materials Selection for Mechanical Design*, 5th ed., Butterworth-Heinemann, 2017.
[10] Homa, J., and Stoltzfus, J. M., "The measurement of the friction coefficient and wear of metals in high-pressure oxygen," Flammability and Sensitivity of Materials in Oxygen-Enriched Atmospheres, Vol. 6, 1993, pp. 389-403.
[11] Gunaji, M., and Stoltzfus, J. M., "Review of frictional heating test results in oxygen-enriched environments," Flammability and Sensitivity of Materials in Oxygen-Enriched Atmospheres, Vol. 6, 1993, pp. 146–156.
[12] Schoenman, L., Stoltzfus, J., and Kazaroff, J., "Friction-Induced Ignition of Metals in High-Pressure Oxygen," Flammability and Sensitivity of Materials in Oxygen-Enriched Atmospheres, Vol. 3, 1988, pp. 105-133.
[13] COMSOL Multiphysics® v. 6.0. www.comsol.com. COMSOL AB, Stockholm, Sweden.
[14] Air Products and Chemicals, Inc., Thermodynamic Data on Oxygen and Nitrogen, ASD-TR-61-625, 1961.
[15] Jenny, R., and Wyssmann, H. R., "Friction-Induced Ignition in Oxygen," Flammability and Sensitivity of Materials in Oxygen-Enriched Atmospheres, Vol. 1, 1983, pp. 150-166.
[16] Benz, F. J., Shaw, R. C., and Homa, J. M., "Burn Propagation Rates of Metals and Alloys in Gaseous Oxygen," Flammability and Sensitivity of Materials in Oxygen-Enriched Atmospheres, Vol. 2, 1986, pp. 135-152.
[17] Wilson, D., and Stoltzfus, J., "Fundamentals of metals ignition in oxygen," Flammability and Sensitivity of Materials in Oxygen-Enriched Atmospheres, Vol. 8, 1997, pp. 272–283.
[18] Lynn, D., Steinberg, T., Sparks, K., Stoltzfus, J. M., Barthelemy, H., and Dean, S. W., "Defining the flammability of cylindrical metal rods through characterization of the thermal effects of the ignition promoter," Journal of ASTM International, Vol. 6, 2009.
[19] Benz, F. J., Shaw, R. C., and Homa, J. M., "Burn propagation rates of metals and alloys in gaseous oxygen," Flammability and Sensitivity of Materials in Oxygen-Enriched Atmospheres, Vol. 2, 1986, pp. 135-152.
[20] Stoltzfus, J. M., Homa, J. M., Williams, R. E., and Benz, F. J., "ASTM committee G-4 metals flammability test program: data and discussion," Flammability and Sensitivity of Materials in Oxygen-Enriched Atmospheres, Vol. 3, 1988, pp. 28-53.
[21] Mcllroy, K., Zawierucha, R., and Dmevich, R. F., "Promoted ignition behavior of engineering alloys in high-pressure oxygen," Flammability and Sensitivity of Materials in Oxygen-Enriched Atmospheres, Vol. 3, 1988, pp. 85-104.
[22] Semenov, N. N., *Chemical kinetics and chain reactions*, Oxford University Press, London, 1935.
[23] Glassman, I., and Yetter, R. A., *Combustion*, 4th ed., Academic Press, 2008.
[24] Bale, C. W., Bélisle, E., Chartrand, P., Decterov, S. A., Eriksson, G., Gheribi, A. E., Hack, K., Jung, I. H., Kang, Y. B., Melançon, J., Pelton, A. D., Petersen, S., Robelin. C., Sangster, J., Spencer, P., and Van Ende, M-A., FactSage Thermochemical Software and Databases - 2010 - 2016, Calphad, Vol. 54, 2016, pp 35-53, <www.factsage.com>